Article ID: 1007-4627(2012)01-0025-11

Energy Spectra of Light Charged Particles and Evaporation Residues in Heavy Ion Induced Reactions at Low Energy

LÜ Qi-wen[1], WEI Hua-rong[1], Rahim Magda A.[2], Fakhraddin S.[2], LIU Fu-hu[1]

(1. *Institute of Theoretical Physics, Shanxi University, Taiyuan* 030006, *Shanxi, China*;
2. *Physics Department, Faculty of Science, Sana'a University, Republic of Yemen*)

Abstract: Using a unified description on multiplicity distributions of final-state particles, the energy spectra of light charged particles and evaporation residues in heavy ion induced reactions at low energy are studied in the framework of a multisource ideal gas model. Each source in an excited composite contributes energy spectra of light charged particles and evaporation residues to be an exponential law. The calculated results are compared and found to be in agreement with the experimental data of inclusive and exclusive energy distributions for light charged particles and evaporation residues measured in the ^{20}Ne (158, 170, 180, and 200 MeV) + ^{12}C reactions.

Key words: unified description; energy spectrum; light charged particle; evaporation residue; excited composite; heavy ion induced reaction

CLC number: O571 **Document code**: A

1 Introduction

It is known that an excited composite is usually formed in light or heavy ion induced reactions at low energy (a few MeV/u). To investigate the properties and behaviors of the excited composite at various stages of the deexcitation cascade process, light charged particles such as protons (p), deuterons (d), tritons (t), and α-particles evaporated from the reactions are widely measured to give their multiplicity distributions, angular distributions, energy spectra, and others. In light ion induced reactions the excited composite gains low excitation energy and low angular momentum, and the energy spectra of light charged particles emitted in such reactions are satisfactorily explained by the statistical model predictions[1−2]. Oppositely, in heavy ion induced reactions the excited composite gains high excitation energy and high angular momentum, and the energy spectra of light charged particles emitted in such reactions are inconsistent with the respective predictions of the statistical model[3]. It is known that in heavy ion induced reactions the high angular momentum induced the deformation of the excited composite. Meanwhile, α-cluster structure in α-like nuclei influence the reaction process and contribute to the deformation of the concerned composite.

As a 5α + 3α system, the ^{20}Ne + ^{12}C system were extensively investigated in recent years[4−6] in connection with the study of nuclear orbiting in α-cluster systems. The deformation of the excited composite formed in the ^{20}Ne + ^{12}C reactions at

Received date: 4 Mar. 2011; **Revised date**: 23 Mar. 2011

Foundation item: National Natural Science Foundation of China(10975095, 11005003); National Fundamental Fund of Personnel Training(J1103210); Shanxi Provincial Natural Science Foundation(2007011005)

Biography: LÜ Qi-wen(1982—), female, Beijing, Ph. D Candidate, working on particle and nuclear physics; E-mail: luqw@ihep.ac.cn

Corresponding author: LIU Fu-hu, E-mail: fuhuliu@163.com; liufh@mail.sxu.cn

7～10 MeV/u was estimated from the study of the respective α-evaporation spectra and found to be much larger than normal deformation in non-α-cluster systems. With emissions of α-particles in the large deformation composite, the emissions of other light particles, such as p, d, and t, in coincidence with individual evaporation residues are also interesting to study and probe the finer details of the reaction mechanism[7－11]. Such studies may enable us to explore the evaporation decay cascade of the composite system and estimate the contributions from fission-like, pre-equilibrium, and other non-evaporative decay channels.

Recently, Dey et al.[12] reported an inclusive and exclusive measurement of (non-evaporative) light charged particles emitted in coincidence with individual evaporation residues of hot (excited) ^{32}S nucleus produced in the $^{20}Ne+^{12}C$ reactions at 7～10 MeV/u. It is obvious that the inclusive and exclusive energy spectra are different from each other. Especially, such exclusive energy data may provide important clues to reveal the intricacies of the decay cascade[12]. At intermediate and high energies, final-state charged particles and nuclear fragments emitted in particle-particle, particle-nucleus and nucleus-nucleus collisions were measured in the past years (e.g. Refs.[13－19]). Multiplicity distributions of charged particles and nuclear fragments, isotropic production cross-sections of nuclear fragments, and other interesting results were reported.

Very recently, we proposed a unified description on multiplicity distributions of final-state particles in different collision systems at high energies[20] and studied the multiplicity distributions and isotopic production cross-sections of nuclear fragments in pA (p-nucleus) and AA (nucleus-nucleus) reactions at intermediate and high energies[21－22] in the framework of our multisource ideal gas model. Although the reaction mechanisms are different at low, intermediate, and high energies, it is expected that our model can be used to describe the energy spectra of light charged particles (light nuclear fragments) and evaporation residues (heavy nuclear fragments) produced in nucleus-nucleus collisions at low energy. In this paper, we shall use the unified description[20] to describe the energy distributions of light charged particles and evaporation residues emitted from the hot composite formed in the $^{20}Ne+^{12}C$ reactions at 7～10 MeV/u[12].

2 The model

In our recent work[20], a unified formula was proposed to describe the multiplicity distributions of final-state particles produced in e^+e^-, pp, $p\bar{p}$, e^+p, pA, and AA collisions at high energies. If we regard the neutron number in a nuclide as the neutron multiplicity-like in a final state, the unified formula can be used to analyze the isotopic production cross-sections of nuclear fragments[21]. It is shown that the model describes also the multiplicity distributions of nuclear fragments in pA and AA collisions[22]. The main idea of our model is that many emission sources of particles and fragments are assumed to be formed in collisions. Each source contributes multiplicity distribution to be an exponential law. If we regard the kinetic energy of a given nuclear fragment as a result of multisource contribution, the unified formula can be used to describe the energy spectra of nuclear fragments. Although the model used in the present work can be found in our recent work[20], we give the model in the following in terms of energy and its distribution for a whole presentation of the present work.

In the model, many emission sources of particles and fragments are assumed to be formed in collisions. According to different interaction mechanisms or event samples, the sources are divided into l groups (sub-samples). The source number in the jth group is assumed to be m_j. Each source contributes energy distribution to be an exponential law, i.e., the energy (E_{ij}) distribution contributed by the ith source in the jth group is

given by

$$P_{ij}(E_{ij}) = \frac{1}{\langle E_{ij}\rangle}\exp\left(-\frac{E_{ij}}{\langle E_{ij}\rangle}\right), \quad (1)$$

where $\langle E_{ij}\rangle = \int E_{ij}P_{ij}(E_{ij})\mathrm{d}E_{ij}$ is the mean energy contributed by the ith source in the jth group, and corresponds to the temperature of the considered source in the model. Generally, we assume $\langle E_{1j}\rangle = \langle E_{2j}\rangle = \cdots = \langle E_{m_j j}\rangle$. The energy ($E_{\mathrm{c.m.}}$) distribution of nuclear fragments in center-of-mass reference system contributed by the jth group is then given by the folding of m_j exponential functions, i.e. we have an Erlang distribution

$$P_j(E_{\mathrm{c.m.}}) = \frac{E_{\mathrm{c.m.}}^{m_j-1}}{(m_j-1)!\langle E_{ij}\rangle^{m_j}}\exp\left(-\frac{E_{\mathrm{c.m.}}}{\langle E_{ij}\rangle}\right). \quad (2)$$

The energy distribution contributed by the l groups is given by a weighted sum of l Erlang distributions

$$P(E_{\mathrm{c.m.}}) = \frac{1}{N}\frac{\mathrm{d}N}{\mathrm{d}E_{\mathrm{c.m.}}} = \sum_{j=1}^{l} k_j P_j(E_{\mathrm{c.m.}}), \quad (3)$$

where N and k_j denote the fragment number and weight factor respectively. Generally, $k_1 + k_2 + \cdots + k_l = 1$.

In the above discussions, m_j denotes the source number in the jth group. To avoid calculation of $(m_j-1)!$ when m_j-1 is too large, we use the Monte Carlo method to calculate the energy distribution of nuclear fragments. Let R_{ij} denote random variable in $[0, 1]$. According to Eq. (1), we have

$$E_{ij} = -\langle E_{ij}\rangle \ln R_{ij}. \quad (4)$$

The fragment energy contributed by the jth group can be obtained by

$$E_{\mathrm{c.m.}} = -\sum_{i=1}^{m_j}\langle E_{ij}\rangle \ln R_{ij}, \quad (5)$$

due to it being the folding of m_j exponential functions. The energy contributed by the l groups is given by a weighted sum

$$E_{\mathrm{c.m.}} = -\sum_{j=1}^{l} k_j \sum_{i=1}^{m_j}\langle E_{ij}\rangle \ln R_{ij}. \quad (6)$$

The energy distribution is finally obtained by a statistical method.

The present model does not answer what the sources are. In the framework of a combination model of constituent quarks and the Landau hydrodynamics[23-24], we may regard the sources as quarks and gluons in the case of m_j being a large value. If m_j is a small value, we may regard the sources as nucleons or nucleon clusters. In the framework of a two-stage gluon model or a gluon dominance model[25-27], the sources can be regarded as active gluons and evaporated gluons.

3 Comparisons with experimental data

The inclusive and exclusive (non-evaporative) spectra for protons emitted in 158 MeV ^{20}Ne+^{12}C reaction at different angles are presented in Fig. 1 by the closed and open circles respectively[12]. In the figure, σ, Ω, and $E(E_{\mathrm{c.m.}})$ denote the cross-section, spherical angle, and kinetic energy, respectively. Fig. 2 shows the measured exclusive proton spectra (circles[12]) emitted in 170 and 200 MeV ^{20}Ne+^{12}C reactions at 10°. The experimental data of Dey et al.[12] are compared with our calculated results (curves). The parameter values obtained by fitting the experimental data are shown in the figures and the values of χ^2 per degree of freedom (χ^2/dof) are given in Table 1, where the unit of $\langle E_{ij}\rangle$ is MeV and the same unit is used in the following figures. One can see that the model describes the experimental data of inclusive and exclusive spectra for protons emitted in ^{20}Ne+^{12}C reactions at 158, 170 and 200 MeV.

The inclusive energy spectra for tritons, deuterons, and protons emitted in ^{20}Ne+^{12}C reactions at different incident energies and emission angles are displayed in Figs. 3, 4, and 5, respectively. The circles and squares indicted by timing different amounts represent the experimental data of Dey et al.[12] at different emission angles. The curves are our calculated results with different parameter values indicated in the figures in terms of

"($\langle E_{i1}\rangle$, m_1)". The corresponding values of χ^2/dof are given in Table 1. Once again the model describes the experimental data of light charged particles.

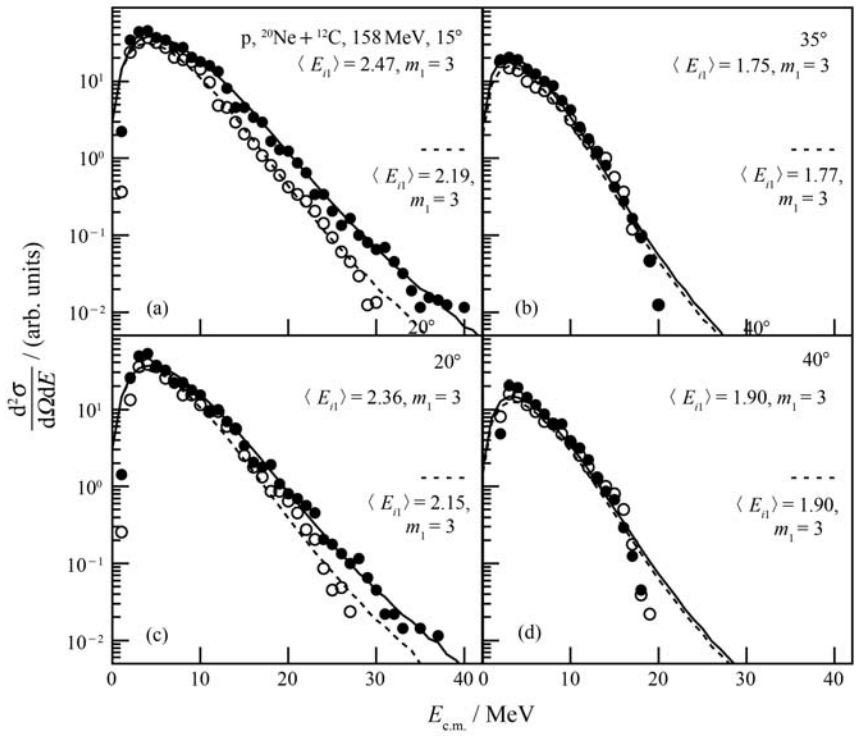

Fig. 1 Inclusive (closed circles and solid curves) and exclusive (open circles and dotted curves) spectra for protons emitted in 158 MeV ^{20}Ne+^{12}C reactions at different angles. The symbols represent the experimental data of Dey et al.[12]. The curves are our calculated results by Eq. (6).

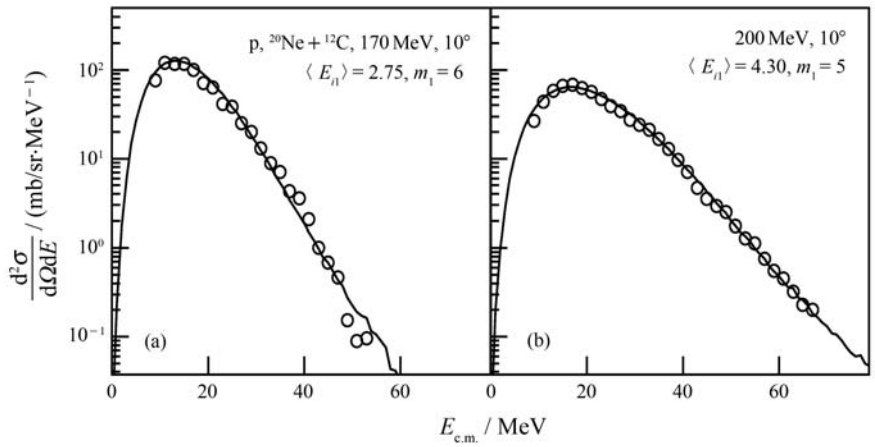

Fig. 2 As for Fig. 1, but showing the measured exclusive proton spectra emitted in 170 and 200 MeV ^{20}Ne+^{12}C reactions at 10°.

Table 1　Values of χ^2/dof corresponding to the fits in Figs. 1～9*

Figure	Type	χ^2/dof	Figure	Type	χ^2/dof
Fig. 1	15°	1.544/1.408	Fig. 5	170 MeV, 50°	1.799
	20°	1.369/1.066		180 MeV, 10°	0.447
	35°	1.590/1.718		180 MeV, 20°	0.400
	40°	1.474/1.337		180 MeV, 30°	0.393
Fig. 2	170 MeV	0.744		180 MeV, 40°	0.712
	200 MeV	0.231		180 MeV, 50°	0.221
Fig. 3	158 MeV, 30°	1.359		200 MeV, 10°	0.663
	158 MeV, 40°	0.818		200 MeV, 20°	0.487
	158 MeV, 50°	1.585		200 MeV, 30°	0.546
	170 MeV, 30°	0.760		200 MeV, 40°	0.733
	170 MeV, 40°	0.596		200 MeV, 50°	0.312
	170 MeV, 50°	1.228	Fig. 6	15°	0.763
	180 MeV, 30°	0.973		20°	1.002
	180 MeV, 40°	0.906		35°	1.563
	180 MeV, 50°	1.080		40°	1.293
	200 MeV, 30°	0.308	Fig. 7	10°	0.970/0.697
	200 MeV, 40°	0.452		20°	1.657/0.684
	200 MeV, 50°	0.892		30°	1.468/0.708
Fig. 4	158 MeV, 30°	1.533		40°	1.209/0.836
	158 MeV, 40°	1.174		50°	1.231/0.717
	158 MeV, 50°	0.619	Fig. 8	α-Ne, 20°	1.700
	170 MeV, 30°	1.469		α-Ne, 40°	0.691
	170 MeV, 40°	1.373		α-Na, 20°	1.429
	170 MeV, 50°	1.141		α-Na, 40°	1.206
	180 MeV, 30°	1.038		p-Na, 20°	1.652
	180 MeV, 40°	1.039		p-Na, 40°	1.320
	180 MeV, 50°	0.936		α-Mg, 20°	0.935
	200 MeV, 30°	1.367		α-Mg, 40°	0.676
	200 MeV, 40°	0.522		p-Mg, 20°	1.662
	200 MeV, 50°	0.882		p-Mg, 40°	0.872
Fig. 5	158 MeV, 10°	1.755		α-Al, 20°	1.333
	158 MeV, 20°	1.014		α-Al, 40°	1.159
	158 MeV, 30°	0.390		p-Al, 20°	1.624
	158 MeV, 40°	0.540		p-Al, 40°	1.516
	158 MeV, 50°	0.496	Fig. 9	Ne	1.596/1.222
	170 MeV, 10°	0.701		Na	1.702/1.713
	170 MeV, 20°	1.475		Mg	1.387/1.743
	170 MeV, 30°	0.948		Al	1.441/1.524
	170 MeV, 40°	1.043			

* The values of χ^2/dof given under "/" are for the dotted curves.

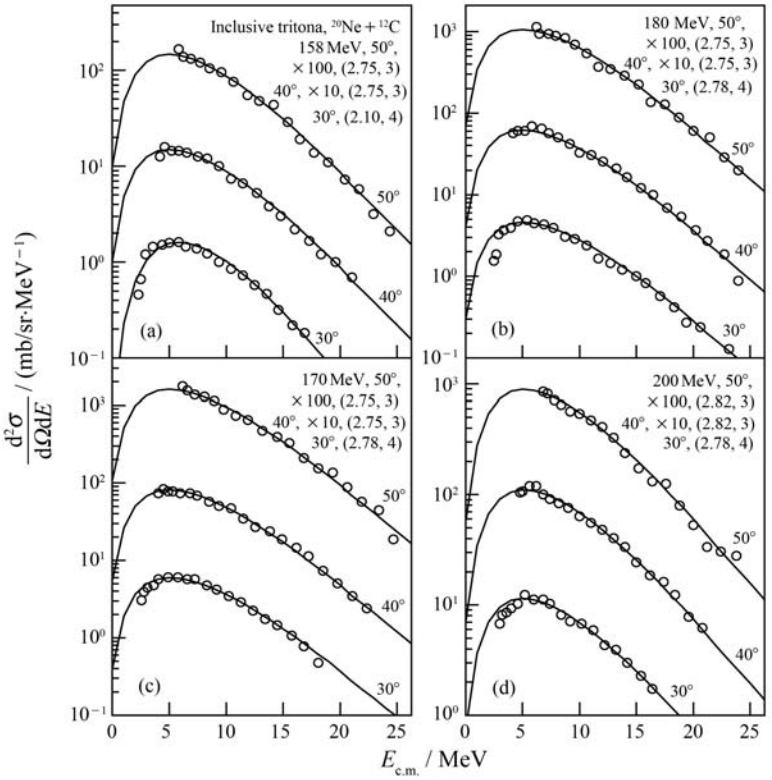

Fig. 3 As for Fig. 1, but showing the inclusive energy spectra for tritons emitted in ^{20}Ne+^{12}C reactions at different angles and energies.

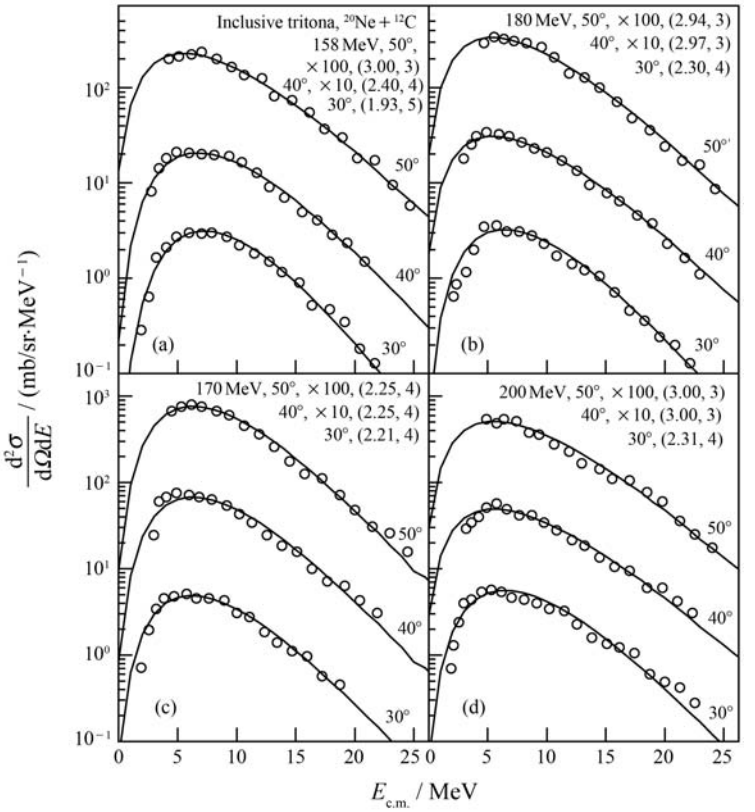

Fig. 4 As for Figs. 1 and 3, but showing the results for deuterons.

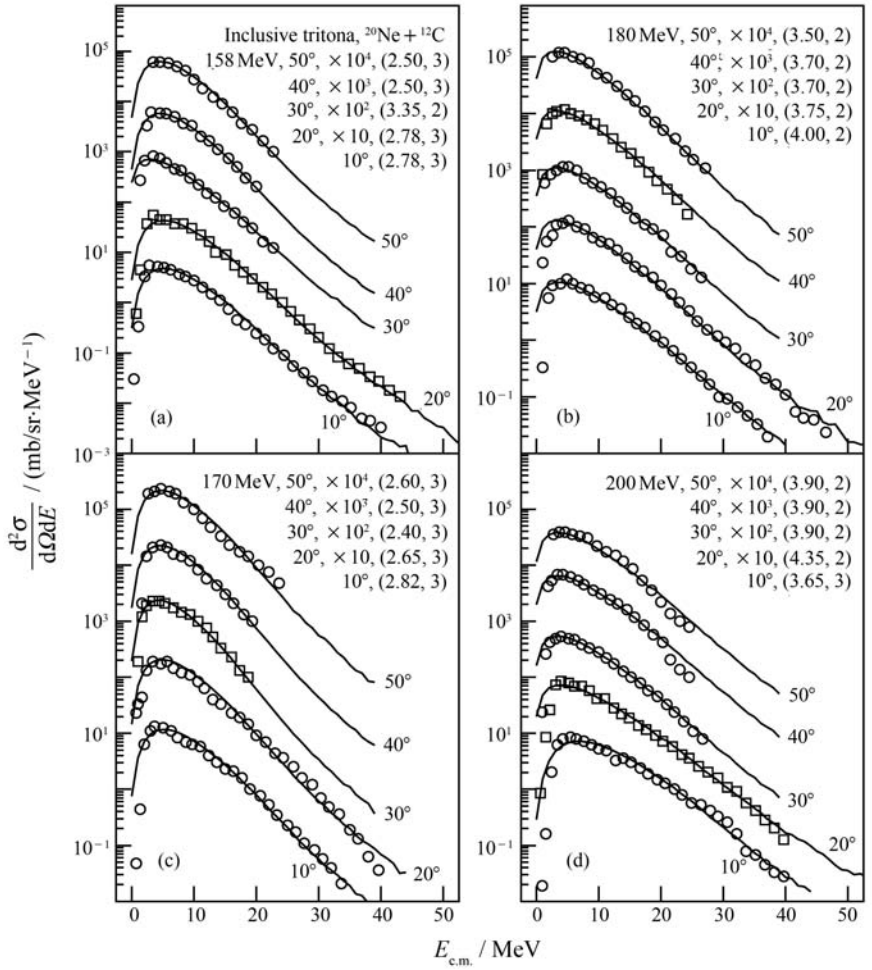

Fig. 5　As for Figs. 1 and 3, but showing the results for protons.

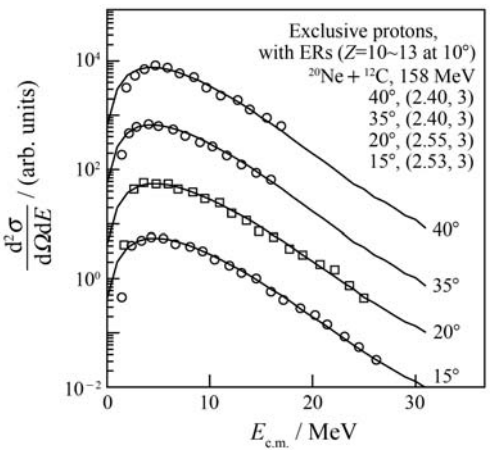

Fig. 6　As for Fig. 1, but showing the exclusive proton spectra at different angles measured in coincidence with ERs (Z = 10 ~ 13) emitted at 10° in 158 MeV ^{20}Ne + ^{12}C reaction.

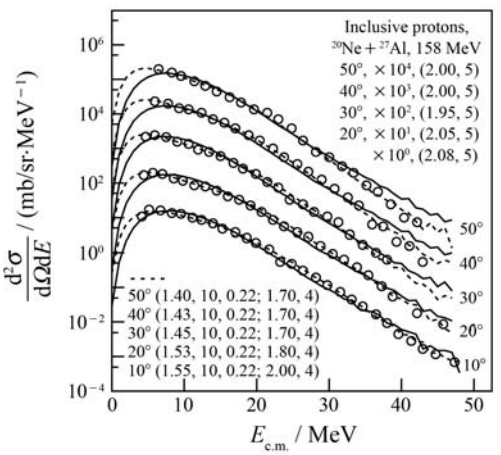

Fig. 7　As for Fig. 1, but showing the inclusive energy spectra for protons emitted in 158 MeV ^{20}Ne + ^{27}Al reaction at different angles.

Fig. 6 presents the exclusive proton spectra at different emission angles measured in coincidence with evaporation residues (ERs with charge $Z=10\sim13$) emitted at 10° in 158 MeV $^{20}Ne+^{12}C$ reaction. Fig. 7 shows the inclusive energy spectra for protons emitted in 158 MeV $^{20}Ne+^{27}Al$ reaction at different emission angles for a comparison. The energy distributions of protons and α-particles at different emission angles measured in coincidence with different evaporation residues at 10° in 158 MeV $^{20}Ne+^{12}C$ reaction are given in Fig. 8. The circles and squares represent the experimental data of Dey et al.[12] and the curves are our calculated results. The parameter values are indicated in the figures in terms of "$(\langle E_{i1}\rangle, m_1)$" or "$(\langle E_{i1}\rangle, m_1, k_1; \langle E_{i2}\rangle, m_2)$". One can see that the model describes the experimental data of light charged particles.

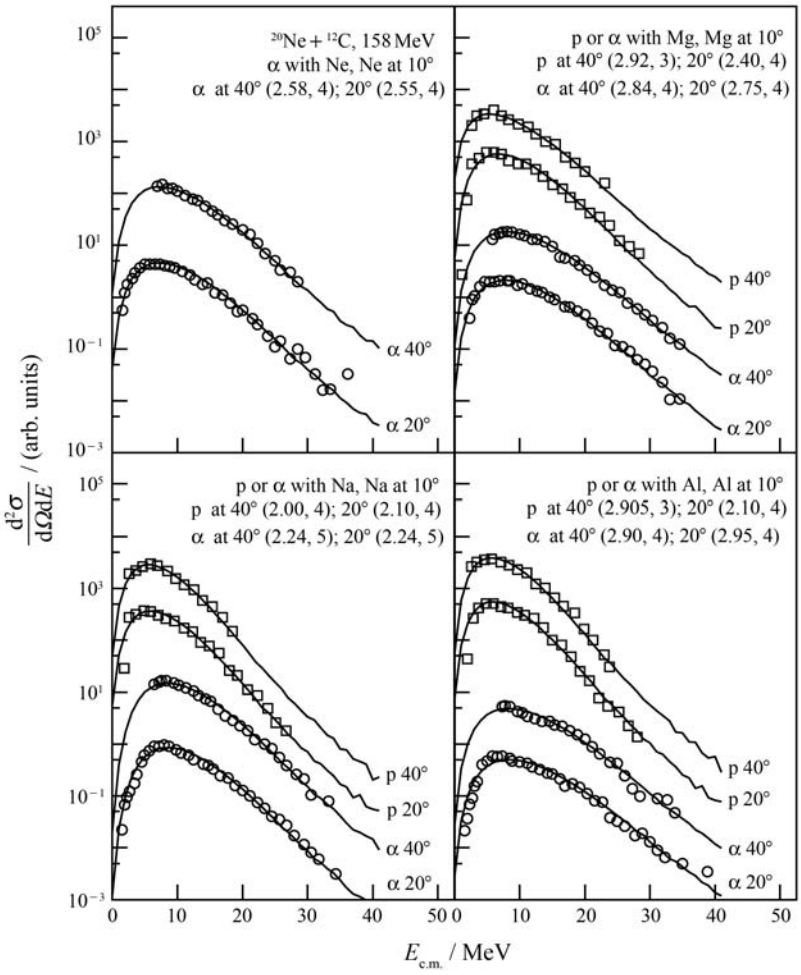

Fig. 8 As for Fig. 1, but showing the inclusive (circles) and exclusive (squares) energy spectra for α-particles and protons at different angles measured in coincidence with different ERs emitted at 10° in 158 MeV $^{20}Ne+^{12}C$ reaction.

The inclusive (higher yields) and exclusive (lower yields) energy spectra for the evaporation residues Ne, Na, Mg, and Al measured in 158 MeV $^{20}Ne+^{12}C$ reaction at 10° are shown in Fig. 9. The undulating lines and the solid (dotted) curves represent the experimental data of Dey et al.[12] and the calculated results of our model respectively. Once again the model describes the experimental data of evaporation residues.

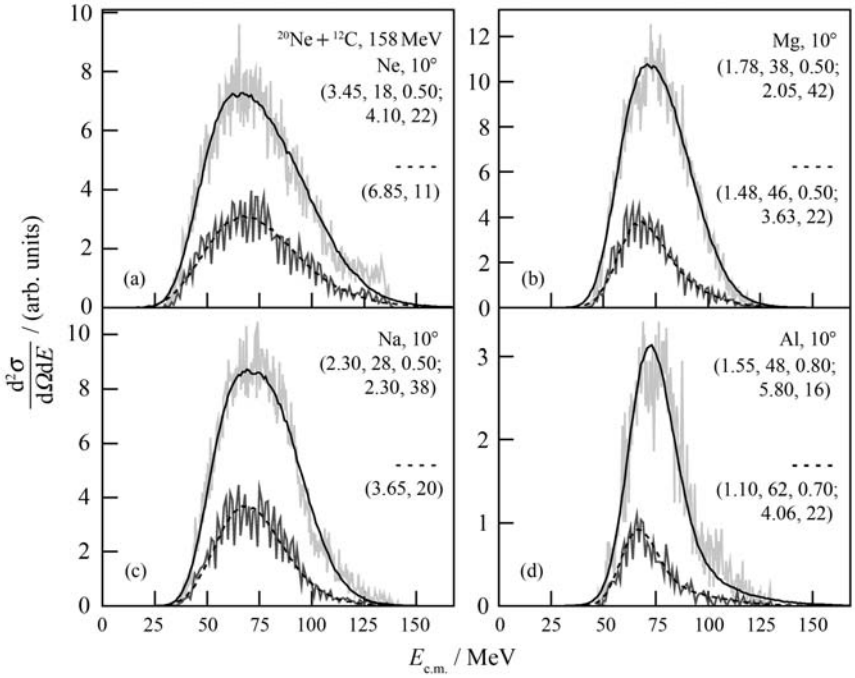

Fig. 9　Inclusive (higher yields) and exclusive (lower yields) energy spectra for different ERs at 10° measured in 158 MeV ^{20}Ne + ^{12}C reaction. The undulating lines represent the experimental data of Dey et al.[12]. The curves are our calculated results.

4　Discussions and conclusions

From the above comparisons, we see that the source numbers for different light charged particles are very small, and these numbers are sometimes different in quantity for different samples. We need only a few sources to give a description for light charged particles. This renders that the sources for light charged particles are nucleons or nucleon clusters which surround the light charged particles in nucleus. These sources stay in a small excitation region in collisions, and are not the light charged particles themselves. A smaller source number corresponds to a smaller excitation region and a lower excitation degree. The light charged particles have only connections with these sources due to the short range property of nuclear force.

We notice that the source numbers for evaporation residues are very large. This renders that the excitation energy remained by light charged and neutral particles is distributed to most or all spectator nucleons, including not only the sources for light charged particles, but also the other spectator nucleons. Mostly, the sources for evaporation residues are nucleons or nucleon clusters. In some cases, the source numbers for evaporation residues are larger than nucleon numbers in collisions. This does not indicate that the quark degrees in some nucleons have contributions to the results. Because the energy scale considered in the present reactions is much smaller in comparison with GeV or TeV energy ranges. The high density region, where hadron-to-quark transition may occur, is not achievable in the present reactions. If the large source number for the produced particles is expected to be related to quark degrees of freedom, the large source number for the evaporation residues is expected to indicate a different physics. In fact, the indication of the large source number for the evaporation residues is still an open question in the present work.

The mean energy can be given by $\sum_{j=1}^{l} k_j \langle E_{ij} \rangle m_j$ which is generally expected to increase with the increases of incident energy and product mass. We

have not found an obvious dependence of $\langle E_{ij} \rangle$ and m_j on the light charged particle mass at the concerned incident energies. For a given kind of light charged particles, e. g. protons, the differences among $\langle E_{i1} \rangle$ as well as m_1 are not essential, but only quantitative, for different samples. The mean value of inclusive spectrum is larger than that of exclusive one. In our opinion, the differences between the two spectra are not essential, too. Our analyses show that the source temperature is a few MeV. This is in agreement with the value obtained from emulsion experiment[28].

The number of free parameters in the model is $3l-1$. We use mostly $l=1$ in the investigation of energy spectra. In a few cases, we have to use $l=2$ due to the contributions of two processes or two sub-samples. It does not always mean that we can get a better result if we use $l=2$ instead of $l=1$. For instance, for the dotted curves in the left panel in Fig. 9, we find that the best result can be obtained by using $\langle E_{i1} \rangle = \langle E_{i2} \rangle$ and $m_1 = m_2$ if we use $l=2$ instead of $l=1$. This means that we describe in fact the data by using $l=1$.

To conclude, the energy distributions of light charged particles and evaporation residues measured in heavy ion induced reactions at 7 ~ 10 MeV/u are studied by using a unified formula. This formula was firstly proposed by us to describe the multiplicity distributions of final-state particles produced in "elementary" particle interactions and heavy ion collisions at high energies. The basis of the formula is a multisource ideal gas model in which each source contributes multiplicity distribution to be an exponential law. The model treats uniformly the final-state particles and nuclear fragments by the same formula. It is shown that the model is successful in the descriptions of multiplicity distributions of different particles and fragments, isotopic production cross-sections of nuclear fragments, and energy spectra of light charged particles and evaporation residues.

Heavy ion reactions are a complex process. Generally, a few fragments are emitted at low energies, and many particles and fragments are emitted at high energy[29-31]. From low to ultrahigh energies, the interaction mechanisms are expected to be different. Meanwhile, one believes that there are commonness laws existing at different energies. The present work is one of the useful attempts in searching for the commonness laws.

References:

[1] VIESTI G, FORNAL B, FABRIS D, *et al*. Phys Rev, 1988, **C38**: 2640.

[2] HUIZENGA J R, BEHKAMI A N, Govil I M, *et al*. Phys Rev, 1989, **C40**: 668.

[3] AWES T C, POGGI G, GELBKE C K, *et al*. Phys Rev, 1981, **C24**: 89.

[4] DEY A, BHATTACHARYA C, BHATTACHARYA S, *et al*. Phys Rev, 2007, **C76**: 034608.

[5] DEY A, BHATTACHARYA S, BHATTACHARYA C, *et al*. Phys Rev, 2006, **C74**: 044605.

[6] BHATTACHARYA C, DEY A, KUNDU S, *et al*. Phys Rev, 2005, **C72**: 021601(R).

[7] GOMEZ D C J, SHAPIRA D, KOROLIJA M, *et al*. Phys Rev, 1996, **C53**: 222.

[8] SHAPIRA D, GOMEZ D C J, KOROLIJA M, *et al*. Phys Rev, 1997, **C55**: 2448.

[9] BHATTACHARYA C, ROUSSEAN M, BECK C, *et al*. Nucl Phys, 1999, **A654**: 841c.

[10] GÓMEZ D CAMPO J, SHAPIRA D, MCCONNELL J, *et al*. Phys Rev, 1999, **C60**: 021601.

[11] BANDOPADHYAY D, BBHATTACHARYA C, KRISHAN K, *et al*. Phys Rev, 2001, **C68**: 064613.

[12] DEY A, BHATTACHARYA S, BHATTACHARYA C, *et al*. Eur Phys J, 2009, **A41**: 39.

[13] WESTFALLl G D, WILSON L W, LINDSTROM P J, *et al*. Phys Rev, 1979, **C19**: 1309.

[14] TSAO C H, SILBERBERG R, BARGHOUTY A F, *et al*. Phys Rev, 1993, **C47**: 1257.

[15] SOLTZ R A, NEWBY R J, KLAY J L, *et al*. Phys Rev, 2009, **C79**: 034607.

[16] DABROWSKA A, SZARSKA M, TRZUPEK A, *et al*. Acta Phys Pol, 2001, **B32**: 3099.

[17] DABROWSKA A, WOSIEK B, WADDINGTON C J. Acta Phys Pol, 2000, **B31**: 725

[18] NAPOLITANI P, SCHMIDT K H, TASSAN-GOT L. arXiv: 0806.3372v1 [nucl-ex], 2008.

[19] BENLLIURE J, FERNÁNDEZ-ORDÓÑEZ M, AUDOUIN L, *et al*. Phys Rev, 2008, **C78**: 054605.
[20] LIU Fuhu. Nucl Phys, 2008, **A810**: 159.
[21] LIU Fuhu, LI Junsheng. Phys Rev, 2008, **C78**: 044602.
[22] LIU Fuhu, LÜ Qiwen, LI Baochun, *et al*. Chin J Phys, 2011, **49**: 601.
[23] SARKISYAN E K G, SAKHAROV A S. arXiv:hep-ph/0410324, 2004.
[24] SARKISYAN E K G, SAKHAROV A S. arXiv:hep-ph/0510191, 2005.
[25] KOKOULIANA E. Acta Phys Pol, 2004, **B35**: 295.
[26] KOKOULINA E S, NIKITIN V A. arXiv:hep-ph/0502224, 2005.
[27] ERMOLOV P F, KOKOULINA E S, KURAEV E A, *et al*. arXiv: hep-ph/0503254, 2005.
[28] LIU Fuhu. High Energy Nuclear Collisions in Nuclear Emulsion[D]. Beijing: China Institute of Atomic Energy, 1993 (in Chinese).
(刘福虎. 原子核乳胶中的高能核碰撞[D]. 北京: 中国原子能科学研究院, 1993.)
[29] YE Yanlin, FAISAL J Q, LOU Jianling, *et al*. Nuclear Physics Review, 2010, **27**(4): 390 (in Chinese).
(叶沿林, FAISAL J Q, 楼建玲, 等. 原子核物理评论, 2010, **27**(4): 390.)
[30] JIANG Zhijin, SUN Yufen. Nuclear Physics Review, 2010, **27**(4): 421 (in Chinese).
(姜志进, 孙玉芬. 原子核物理评论, 2010, **27**(4): 421.)
[31] MA Ke, ZHU Guangxi, ZHOU Daicui. Nuclear Physics Review, 2010, **27**(4): 426.

低能重离子诱导反应中轻带电粒子和蒸发剩余物的能谱

吕绮雯[1], 卫华荣[1], Rahim Magda A.[2], Fakhraddin S.[2], 刘福虎[1]
(1. 山西大学理论物理研究所, 山西 太原 030006;
2. 萨那大学理学院物理系, 萨那, 也门共和国)

摘要: 在多源理想气体模型的框架内, 用一个关于末态粒子多重数分布的统一描述, 研究了低能重离子诱导反应中轻带电粒子和蒸发剩余物的能谱。在同一个激发的复合核中, 每个源对带电粒子和蒸发剩余物均贡献一个指数分布的能谱。计算结果与 158, 170, 180 和 200 MeV $^{20}Ne+^{12}C$ 反应中, 轻带电粒子和蒸发剩余物能谱的实验结果符合。

关键词: 统一描述; 能谱; 轻带电粒子; 蒸发剩余物; 激发了的复合核; 重离子诱导反应

收稿日期: 2011-03-04; **修改日期**: 2011-03-23
基金项目: 国家自然科学基金资助项目(10975095, 11005003); 国家基础科学人才培养基金资助项目(J1103210); 山西省自然科学基金资助项目(2007011005)
通讯联系人: 刘福虎, E-mail: fuhuliu@163.com; liufh@mail.sxu.cn